PROCEEDINGS OF SCIENCE

Measurement of cosmic-ray proton and helium spectra from the ISS-CREAM experiment

G. H. Choi[a,g,*] **and E. S. Seo**[b,c] **on behalf of the ISS-CREAM collaboration**

[a] *Dept. of Physics, Sungkyunkwan University, Republic of Korea*
[b] *Inst. for Phys. Sci. and Tech., University of Maryland, College Park, MD, USA*
[c] *Dept. of Physics, University of Maryland, College Park, MD, USA*
[g] *Korea Aerospace Research Institute, Daejeon, Republic of Korea*

E-mail: chgwangho@kari.re.kr, seo@umd.edu

The Cosmic Ray Energetics And Mass for the International Space Station (ISS-CREAM) experiment successfully recorded data for 539 days from Aug. 2017 to Feb. 2019. The ISS-CREAM instrument consists of a Silicon Charge Detector (SCD), carbon targets, a calorimeter (CAL), a top counting detector (TCD), a bottom counting detector (BCD), and a boronated scintillator detector (BSD). In this analysis, the SCD was used for the charge measurements. It comprises four layers, and each SCD layer is finely segmented with 2,688 silicon pixels to minimize charge misidentification due to the backscattered particles. The CAL was used for the energy measurements. It comprises 20 layers of tungsten/scintillating fibers. Each tungsten/scintillating-fiber layer consists of a 50 cm × 50 cm × 3.5 mm tungsten plate, followed by a layer of fifty 1 cm-wide 50 cm-long scintillating-fiber ribbons. The CAL also provides the incident cosmic-ray track and the high-energy trigger. For the low-energy trigger, the TCD and BCD were used. In this paper, we present the proton spectrum from the ISS-CREAM experiment in the energy range of 1.6 - 655 TeV and the preliminary helium spectrum in the energy range of 2.7 TeV - 1.1 PeV.

38th International Cosmic Ray Conference (ICRC2023)
26 July - 3 August, 2023
Nagoya, Japan

*Speaker

PoS(ICRC2023)108

1. Introduction

The ISS-CREAM payload was launched as part of the 12th Commercial Resupply (CRS-12) mission on August 14, 2017, aboard a SpaceX Falcon 9 rocket from NASA's Kennedy Space Center. The ISS-CREAM payload arrived at the ISS, and it was installed on the ISS of the Japanese Experiment Module Exposed Facility (JEM-EF) #2 on August 21, 2017 [1], as shown in Fig. 1(a). The ISS-CREAM experiment was designed to measure cosmic rays from protons to iron nuclei in the energy range from approximately 1 TeV to 1 PeV. The ISS-CREAM instrument comprises a silicon charge detector (SCD), carbon targets (C-targets), a calorimeter (CAL), a top counting detector (TCD), a bottom counting detector (BCD), and a boronated scintillator detector (BSD), as illustrated in Fig. 1(b).

At the top of the payload, the four-layer SCD is located for charge measurements. Each layer covers an active detection area of 78.2 × 73.6 cm, and it is finely segmented with 2688 silicon pixels. These finely segmented pixels reduce background contamination from backscattered particles coming from detectors located below [2]. C-targets are placed just below the SCD and consist of two high-density graphite blocks. They induce hadronic interactions to generate hadronic showers in the calorimeter [3]. The CAL consists of 20 layers of tungsten/scintillating fibers, and it provides particle energy measurements. The total energy deposited in the scintillating fibers determines the incident cosmic-ray energy, and the CAL can determine the direction of cosmic rays through shower axis reconstruction using the deposited signals in CAL [3]. The top counting detector (TCD) and bottom counting detector (BCD) with segmented photodiodes are placed above and below the CAL, respectively. TCD and BCD (TCD/BCD) provide additional layers to measure the longitudinal and lateral shower profiles. Thus, the TCD/BCD can help distinguish electrons and protons using different shower shapes [4]. Additionally, TCD/BCD provide a low-energy trigger. At the bottom of the instrument is the boronated scintillator detector (BSD), which can provide additional electron/hadron separation by measuring late signals from thermal neutrons [5].

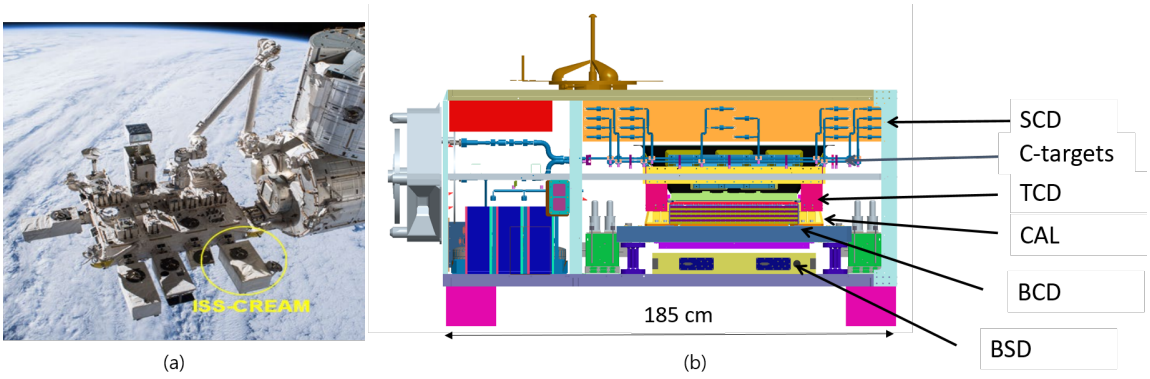

Figure 1: The ISS-CREAM payload was installed on the JEM-EF #2 (a) and its overview (b).

2. Data analysis

The ISS-CREAM instrument has two physics triggers provided by the CAL and TCD/BCD. The CAL provides a high-energy trigger (EHI) that requires each of any six consecutive layers in the

CAL to have at least one ribbon with deposited energy above the threshold [6]. All selected events were triggered by EHI or ELO. Noninteracting particles or particles with the first interaction below the CAL's first layer (late interactions) were removed. These events could result in underestimating the deposited energy in the CAL or misidentifying the incident charge due to the large uncertainty of the trajectory reconstruction [7].

2.1 Trajectory reconstruction

The trajectory of an incident cosmic ray is determined by reconstructing its shower axis within CAL. To reconstruct the shower axis, the largest signal in each layer in the XZ and YZ planes of the CAL is selected. In both XZ and YZ planes, the layer with the highest signal and its nearest two layers are selected for a linear fit. The shower axis of an incident cosmic ray is reconstructed by a chi-squared fit of a straight line through these selected layers [7]. Four combinations of three selected layers are used as an initial fit: layers 1 and 2, 2 and 3, 3 and 1, and all three layers. Extending this fit to the top and bottom layers of the CAL results in the initial shower axis reconstruction. The first selection threshold requires the largest signal within each layer within ± 3 cm of the X (X–Z plane) and Y (Y–Z plane) from the initial shower axis. If the largest signal in the layer within this ± 3 cm range, the layer is selected for the second fit. The final fit is determined by selecting the second fit with the largest number of layers. The slope of this final fit is then compared with the slopes from the four initial fits. It is required for the sign of the slope between the final fit and at least one of the four initial fits to be consistent [7].

Figure 2 is an example of a shower axis reconstruction in the XZ plane of an event, where the red line is the final fit using the selected layers marked with red circles. The largest signal ribbons in each layer are indicated by × symbols.

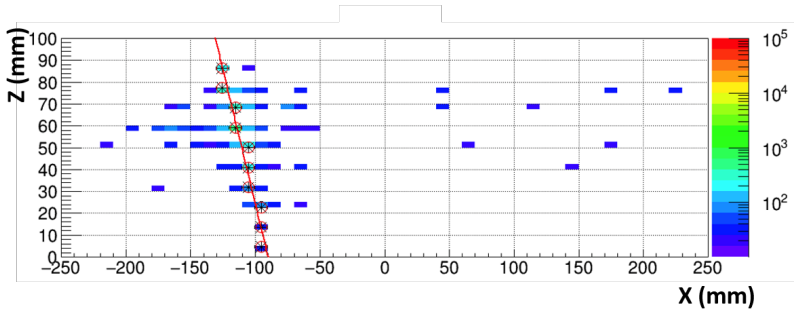

Figure 2: An illustration of the shower axis reconstruction in CAL. The deposited energy in each ribbon is color coded. The largest signal in each layer is indicated with an × symbol, and the circled crosses represent included in the final fit (red line) [7].

2.2 Charge measurement

The reconstructed shower axis of CAL is extrapolated to SCD to determine an incident particle. Within an 11 × 11 pixel area centered on the extrapolated CAL shower axis, the SCD pixels are scanned to find an incident particle. Among these scanned pixels, the one with the highest signal is chosen to identify the incident particle. The signal from the selected pixel is corrected for the particle's path length, calculated from the reconstructed incidence angle of the sensor [7].

Figure 3(a) shows the measured charge histogram with proton and helium nuclei in the top, second, and third layers of the SCD. The statistics of the third layer are lower due to the deactivation of one quadrant after August 2018 [8]. For this analysis, the top layer of the SCD was used to maximize statistics. The measured proton and helium histograms are fitted using a double Landau distribution, and the results of these fits are presented in Fig. 3(b) [7]. The peaks corresponding to proton and helium nuclei are at Z = 0.95 and Z = 2.03, respectively. The corresponding charge resolutions for proton and helium nuclei are 0.14 e and 0.15 e, respectively. The charge-selection ranges for protons and helium are $0.7 < Z < 1.7$ and $1.7 < Z < 2.7$, respectively. For the helium selection, the background subtraction and its corrections are not applied yet.

2.3 Spectral deconvolution

The total deposited energy is determined by summing the deposited energy in all scintillating-fiber ribbons of CAL. Details of the energy calibration of CAL can be found in Zhang et al. 2021 [9] and references therein. The selected protons and helium are counted in each energy bin. The energy bin size was determined by the statistical root-mean-square (rms) resolution of the energy distributions in the CAL. Due to the finite energy resolutions, event counts in energy bins must be corrected for overflows from neighboring bins. This unfolding procedure requires to solve a linear equation. This linear equation converts the measured counts, $N_{dep,j}$, in deposited energy bin j to the counts, $N_{ini,i}$, in incident energy bin i. The conversion matrix [6] used is given in Equation 1:

$$N_{inc,i} = \sum_j P_{i,j} N_{dep,j}, \tag{1}$$

where the matrix element $P_{i,j}$ is the probability that events in the incident energy bin i are from deposited energy bin j. The matrix element $P_{i,j}$ for protons and helium is generated from the protons and helium MC simulation data. The corresponding deconvolution matrix for the protons is described in G. H. Choi and E. S. Seo et al. [7]. The preliminary deconvolution matrix for helium is shown in Fig. 4.

2.4 Absolute flux

The absolute flux, F, is obtained by correcting the measured cosmic rays for the geometrical acceptance, live-time, efficiencies, and backgrounds using Equation 2:

$$F = \frac{dN}{dE} \times \frac{(1-\delta)}{GF \times \varepsilon \times T}, \tag{2}$$

where dN is the number of events in the energy bin size of dE. GF is the geometrical acceptance, T is the live-time, ε is the overall efficiency, and δ is the charge-misidentified fraction caused by backscattered particles. The GF (0.27 ± 0.01 m^2 sr) is obtained by considering the incident particle's traversal through the active regions of both the top layer of the SCD and the BCD. The T is estimated to be 19,753,632 seconds, excluding the routine periodic calibration time and instrument dead-time [7]. ε includes all of the efficiencies, i.e., trigger efficiency, late-interaction efficiency, trajectory-reconstruction efficiency, accuracy of trajectories, charge-selection efficiency, and SCD-active-area efficiency.

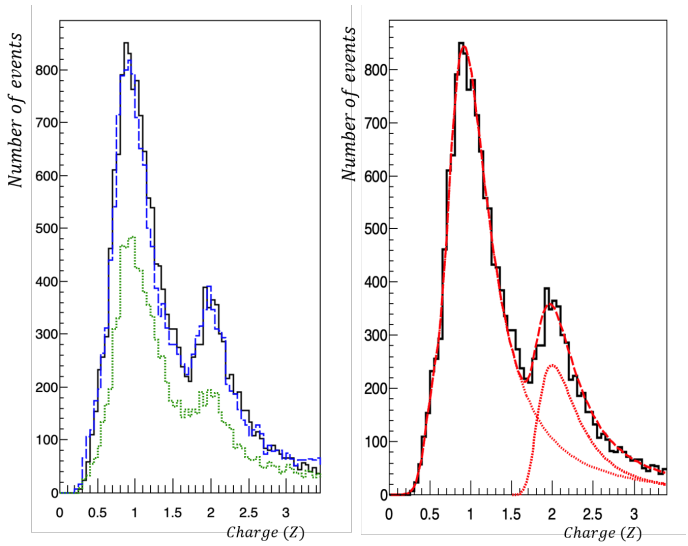

(a) (b)

Figure 3: The measured charge distributions of proton and helium nuclei (a) for each layer (black solid line, top layer; blue dashed line, second layer; green dotted line, third layer) and (b) for the top layer with a double Landau-distribution fit (red dashed line). The red dotted lines represent distributions of each component of the proton and helium nuclei for this fit [7].

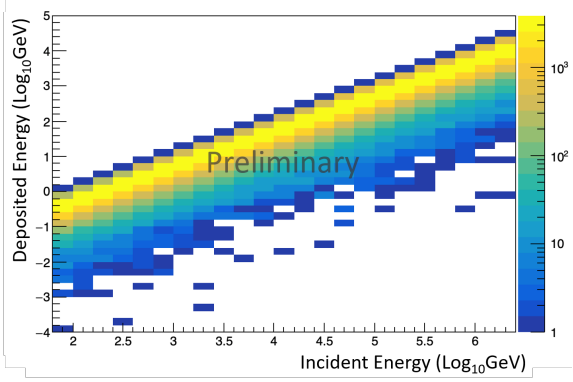

Figure 4: The deconvolution matrix for helium.

3. Results

3.1 Proton and helium spectra

The ISS-CREAM protons are measured in the energy range of 1.6 to 655 TeV. Figure 5 shows the ISS-CREAM proton spectrum as a function of incident energy. The ISS-CREAM proton spectrum is compared with recent experiments [7]: AMS-02 [10–12], CREAM-I+III [6], DAMPE [13], CALET [14], and NUCLEON [16]. The absolute fluxes are multiplied by $E^{2.6}$.

A Smoothly Broken Power law (SBPL) function is used to fit the ISS-CREAM proton spectrum, as given in Equation 3:

$$\Phi(E) = \Phi_0 \left(\frac{E}{E_0}\right)^{-\gamma} \left(1 + \left(\frac{E}{E_b}\right)^{\frac{\Delta\gamma}{\beta}}\right)^{-\beta} (m^2\ sr\ s\ GeV)^{-1} \quad (3)$$

where Φ_0 and E_0 are the initial parameters of flux and energy, respectively. A smooth-fitting parameter, β, is the transition of the power-law indices, γ, below the break energy of E_b to $\gamma + \Delta\gamma$ above E_b. We investigated several SBPL fittings [7] by changing the upper limit of the fit energy range, and these fit results are compared with the single power-law fit with significance. Our SBPL fitting result for the energy range of 1.6 TeV - 164 TeV shows that the ISS-CREAM proton spectrum softens at the break energy of 9.0 ± 1.3 TeV. The power-law indices below and above the break energy are 2.57 ± 0.03 and 2.82 ± 0.02, respectively. As the upper limit of the fitted energy range increases, the significance decreases. It indicates the spectral softening does not continue above 164 TeV [7]. More details of the SBPL fittings are described in G. H. Choi and E. S. Seo et al. 2022 [7].

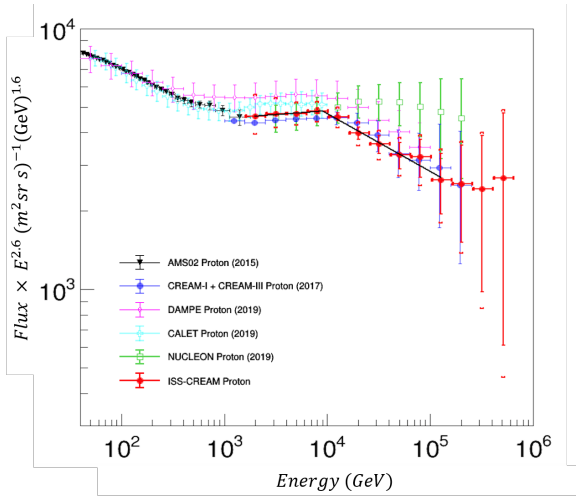

Figure 5: The proton spectrum of the ISS-CREAM experiment is compared with recent data from other experiments. The error bars represent statistical uncertainties, and brackets are obtained by summing the statistical and systematic uncertainties in quadrature for the ISS-CREAM proton spectrum. The black line is the SBPL fit result from the energy range of 1.6 – 164 TeV [7].

Figure 6 shows the preliminary helium spectrum of the ISS-CREAM experiment as a function of incident energy in the energy range of 2.7 TeV - 1.1 PeV. The helium spectrum is dN/dE divided by GF and live-time. The values of GF and live-time were used to 0.27 ± 0.01 m^2 sr and 19,753,632 seconds, respectively. This spectrum will be corrected for efficiency and background to get the absolute flux.

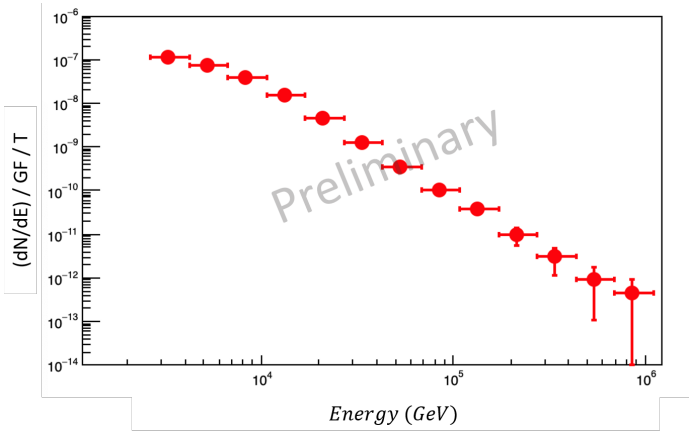

Figure 6: The Preliminary helium spectrum of the ISS-CREAM experiment.

Acknowledgments

This work was supported in the U.S. by NASA grant NNX17AB41G, in Korea by National Research Foundation grants 2022R1F1A1060075 and 2021R1A2B5B03002645, and their predecessor grants, in France by IN2P3/CNRS and CNES, and in Mexico by DGAPA-UNAM project IN109617. The authors thank NASA GSFC WFF and its contractors for engineering support and project management, the JSC ISS Program Office for launch support and ISS accommodation, MSFC for operational support, and KSC and SpaceX for launch support. This work was also supported by the Ministry of Science and ICT, Korea, under the High-Potential Individuals Global Training Program (2021-0-01544) supervised by the IITP (Institute for Information & Communications Technology Planning & Evaluation).

References

[1] E. S. Seo et al., Cosmic Ray Energetics And Mass for the International Space Station (ISS-CREAM), ASR, 53, 1451-1455 (2014).

[2] I. H. Park et al., Silicon charge detector for the CREAM experiment, Nucl. Instrum. Methods Phys. Res. A., 570, 286 (2007)

[3] H. S. Ahn et al., The Cosmic Ray Energetics And Mass (CREAM) instrument, Nucl. Instrum. Methods Phys. Res. A, 579, 1034-1053 (2007)

[4] S. C. Kang et al., On-orbit performance of the top and bottom counting detectors for the ISS-CREAM experiment on the international space station, Nucl. Adv. Space Res., 64, 2564-2569 (2019)

[5] Y. Amare et al., The Boronated Scintillator Detector of the ISS-CREAM Experiment, Nucl. Instrum. Methods A, 943, 162413 (2019)

[6] Y. S. Yoon et al., Proton and helium spectra from the CREAM-III flight, ApJ, 839, 5 (2017)

[7] G. H. Choi and E. S. Seo et al., Measurement of High-energy Cosmic-Ray Proton Spectrum from the ISS-CREAM Experiment, ApJ., 940, 107 (2022)

[8] G. H. Choi et al., On-orbit performance of the ISS-CREAM SCD, PoS(ICRC2019)048 (2019)

[9] H. G. Zhang et al., Performance of the ISS-CREAM calorimeter in a calibration beam test, Astropart. Phys., 23 (2021)

[10] M. Aguilar et al., Precision Measurement of the Proton Flux in Primary Cosmic Rays from Rigidity 1 GV to 1.8 TV with the Alpha Magnetic Spectrometer on the International Space Station, Phy. Rev. Lett. 114, 171103 (2015)

[11] M. Aguilar et al., Observation of the Identical Rigidity Dependence of He, C, and O Cosmic Rays at High Rigidities by the Alpha Magnetic Spectrometer on the International Space Station, Phy. Rev. Lett. 117, 251101 (2017)

[12] M. Aguilar et al., Properties of Neon, Magnesium, and Silicon Primary Cosmic Rays Results from the Alpha Magnetic Spectrometer, Phy. Rev. Lett. 124, 211102 (2020)

[13] DAMPE Collaboration, Measurement of the cosmic ray proton spectrum from 40 GeV to 100 TeV with the DAMPE satellite, Science Advances, 5, 9 (2019)

[14] O. Adriani et al., Direct Measurement of the Cosmic-Ray Proton Spectrum from 50 GeV to 10 TeV with the Calorimetric Electron Telescope on the International Space Station, Phy. Rev. Lett. 122, 181102 (2019)

[15] E. Atkin et al., New Universal Cosmic-Ray Knee near a Magnetic Rigidity of 10 TV with the NUCLEON Space Observatory, JETP LETT, 108, 5 (2018)

[16] V. Grebenyuk et al., Energy spectra of abundant cosmic-ray nuclei in the NUCLEON experiment, Adv. Space Res., 12, 64 (2019)

Full Authors List: ISS-CREAM Collaboration

S. Aggarwal[b,c], Y. Amare[b], D. Angelaszek[b,c], D. Bowman[c], G. H. Choi[a,g], Y. C. Chen[b,c], M. Copley[b], L. Derome[d], L. Eraud[d], C. Falana[b], A. Gerrety[b], J. H. Han[b], H. G. Huh[b], A. Haque[b,c], Y. S. Hwang[e], H. J. Hyun[e], H. B. Jeon[e], J. A. Jeon[a], S. Jeong[a], S. C. Kang[e], H. J. Kim[e], K. C. Kim[b], M. H. Kim[b], M. J. Lee[a], H. Y. Lee[a], J. Lee[e], M. H. Lee[b], L. Lu[b], J. P. Lundquist[b], L. Lutz[b], A. Menchaca-Rocha[f], O. Ofoha[b], H. Park[e], I. H. Park[a], J. M. Park[e], N. Picot-Clemente[b], R. Scrandis[b,c], E. S. Seo[b,c], J. R. Smith[b], R. Takeishi[a], N. Vedenkin[a], P. Walpole[b], R. P. Weinmann[b], H. Wu[b,c], J. Wu[b], Z. Yin[b,c], Y. S. Yoon[b,c], and H. G. Zhang[b]

[a] Dept. of Physics, Sungkyunkwan University, Republic of Korea

[b] Inst. for Phys. Sci. and Tech., University of Maryland, College Park, MD, USA

[c] Dept. of Physics, University of Maryland, College Park, MD, USA

[d] Laboratoire de Physique Subatomique et de Cosmologie, Grenoble, France

[e] Dept. of Physics, Kyungpook National University, Republic of Korea

[f] Instituto de Fisica, Universidad Nacional Autónoma de Mexico, Mexico

[g] Korea Aerospace Research Institute, Daejeon, Republic of Korea

S. C. Kang and Y. S. Yoon are currently affiliated with the Korea Research Institute of Standards and Science in Daejeon, Republic of Korea.

J. A. Jeon, H. Y. Lee, and M. H. Lee are currently affiliated with Institute for Basic Science in Daejeon, Republic of Korea.